

# The Electron Capture Decay of $^{163}\text{Ho}$ to Measure the Electron Neutrino Mass with sub-eV Accuracy

Massimiliano Galeazzi<sup>a</sup>, Flavio Gatti<sup>b</sup>, Maurizio Lusignoli<sup>c</sup>, Angelo Nucciotti<sup>d</sup>, Stefano Ragazzi<sup>d</sup>, Maria Ribeiro Gomes<sup>e</sup>

<sup>a</sup>University of Miami, 1320 Campo Sano Dr., Coral Gables, FL 33146, USA

<sup>b</sup>INFN-Genova and Università degli Studi di Genova, Via Dodecanneso 33, 16146 Genova, Italy

<sup>c</sup>INFN-Roma and Università di Roma La Sapienza, Piazzale Aldo Moro 5, 00185 Roma, Italy

<sup>d</sup>INFN-Milano Bicocca and Università di Milano Bicocca, Piazza della Scienza 3, 20126 Milano, Italy

<sup>e</sup>Centro de Física Nuclear da Universidade de Lisboa, Av. Prof. Gama Pinto, 2, 1649-003, Lisboa, Portugal

---

## Abstract

We have investigated the possibility of measuring the electron neutrino mass with sub-eV sensitivity by studying the electron capture decay of  $^{163}\text{Ho}$  with cryogenic microcalorimeters. In this paper we will introduce an experiment's concept, discuss the technical requirements, and identify a roadmap to reach a sensitivity of  $0.1 \text{ eV}/c^2$  and beyond.

*Keywords:* electron neutrino mass, electron capture decay,  $^{163}\text{Ho}$

---

## 1. Introduction

Assessing the neutrino mass scale is one of the major challenges in today particle physics and astrophysics. Although neutrino oscillation experiments have clearly shown that there are at least three neutrinos with different masses, their absolute values remain unknown. Neutrino flavor oscillations are sensitive to the difference between the squares of neutrino mass eigenvalues and have been measured by solar, atmospheric, reactor, and accelerator experiments [1]. Combining such results, however, does not lead to an absolute value for the eigenmasses, and a dichotomy between two possible scenarios, dubbed "normal" and "inverted" hierarchies, exists. The scenario could be complicated further by the possible existence of additional "sterile" neutrino eigenvalues at different mass scales [2].

The value of the neutrino mass has many implications, from cosmology to the Standard Model of particle physics. In cosmology the neutrino mass affects the formation of large-scale structure in the universe. In particular, neutrinos tend to damp structure clustering, before they have cooled sufficiently to become non-relativistic, with an effect that is dependent on their mass [3]. In the framework of  $\Lambda$ -CDM cosmology, the scale dependence of clustering observed in the Universe can, indeed, be used to set an upper limit on the neutrino mass sum in the range between about 0.3 and 2 eV [4], although this

value is strongly model-dependent. In particle physics, a determination of the absolute scale of neutrino masses would help shedding light on the mechanisms of mass generation.

For years, laboratory experiments based on the study of proper nuclear processes have been used to directly measure the neutrino masses. In particular, single beta decay has been, historically, the traditional and most direct method to investigate the electron (anti)neutrino mass [5]. Neutrinoless double beta decay has also been suggested as a powerful tool to measure the electron neutrino mass, although the decay itself, and thus its efficacy at measuring the neutrino mass, is dependent on the assumption that the neutrino is, in fact, a Majorana particle [6].

To date, the study of the beta decay of  $^3\text{H}$  using electrostatic spectrometers has been the most sensitive approach, yielding an upper limit on the electron anti-neutrino mass of  $2.2 \text{ eV}/c^2$  [7]. In the near future, the new experiment KATRIN will analyze the  $^3\text{H}$  beta decay end-point with a much more sensitive electrostatic spectrometer and an expected statistical sensitivity of about  $0.2 \text{ eV}/c^2$  [8].

The calorimetric measurement of the beta decay of  $^{187}\text{Re}$  using cryogenic microcalorimeters has also been successfully used [9], and a new experiment, MARE, is planned to have a sensitivity for the neutrino mass comparable to that of KATRIN [10]. Although a calorimet-

ric experiment is not affected by the many systematic uncertainties that plagued electrostatic spectrometers in the past, the very nature of the experiments requires that all decays are being measured, not only those with energy near to the end-point. To maximize the useful experimental statistics, a calorimetric experiment thus requires an isotope with very low end-point energy, hence the choice of  $^{187}\text{Re}$ , with an end-point energy of about 2.5 keV [9].

The potential of MARE is quite promising and its first phase is well under way. However, its full implementation and, more important, its extension beyond the  $0.2\text{ eV}/c^2$  limit currently planned, are strongly affected by the long decay time of  $^{187}\text{Re}$ . With a half-life comparable to the age of the Universe – about  $43 \times 10^9$  years [9] –, the mass of radioactive material necessary to reach the high statistics required by the experiment in a reasonable amount of time puts serious constraints on the experimental design and fabrication [11].

It was suggested thirty years ago that electron capture (EC) decays with low  $Q$ -values could be used as an alternative to single beta decay for the direct determination of the electron neutrino mass. In 1981 a group at Princeton University [12] tried to obtain a limit on the electron neutrino mass measuring the X-rays emitted after EC of electrons in different levels. In the same year De Rújula [13] proposed to measure the spectra of photons emitted by inner brehmsstrahlung in EC decays (IBEC) with the K shell capture forbidden, and an experimental activity followed [14]. The spectrum of emitted Auger electrons was also considered later [15]. The most appealing suggestion, that we will follow in this Letter, considers a calorimetric experiment, where all the de-excitation energy is recorded [16].

The EC decay of  $^{163}\text{Ho}$  to  $^{163}\text{Dy}$  is the decay with the lowest known  $Q$ -value and its half-life of a few thousand years is much less than the  $^{187}\text{Re}$  one. Detailed theoretical calculations and sensitivity to the neutrino mass in the  $^{163}\text{Ho}$  case are reported in [16]. In 1997 the  $^{163}\text{Ho}$  decay was measured using cryogenic microcalorimeters [17] and in 2008 its use was suggested included in the framework of the MARE experiment [18]. More recently, a similar, parallel effort with magnetic microcalorimeters has also started [19]. Unfortunately, at this time the experimental measurements of the  $Q$ -value range from about 2.2 keV to 2.8 keV, an uncertainty that translates to a factor 3 to 4 on the neutrino mass sensitivity achievable by a Holmium experiment.

In this paper we discuss the potential of an experiment to measure the electron neutrino mass with sub-eV sensitivity by studying the electron capture decay of

$^{163}\text{Ho}$  with cryogenic microcalorimeters. In particular, we will introduce the experiment's concept, discuss the technical requirements, and identify a roadmap to reach a sensitivity of  $0.1\text{ eV}/c^2$  and beyond.

## 2. Measuring the electron neutrino mass through the $^{163}\text{Ho}$ electron capture decay

There are at least three proposed independent methods to assess the neutrino mass from the  $^{163}\text{Ho}$  EC decay:

1. Absolute M capture rates or M/N capture rate ratios [12];
2. Inner Bremsstrahlung (IB) end-point [13];
3. Total (calorimetric) absorption spectrum end-point [16].

### *Absolute M capture rates or M/N capture rate ratios*

All the experimental research so far has focused on the atomic emissions - photons and electrons - following the EC to exploit the possibility of constraining simultaneously the transition  $Q$  and the neutrino mass from the relative probabilities of M and N shell capture or absolute M capture rate [12, 20, 21].

The EC decay rate can be expressed, following [22], as a sum over the possible levels of the captured electron:

$$\lambda_{EC} = \frac{G_{\beta}^2}{4\pi^2} \sum_i n_i C_i \beta_i^2 B_i \times (Q - E_i)[(Q - E_i)^2 - m_{\nu}^2]^{1/2}, \quad (1)$$

where  $G_{\beta} = G_F \cos \theta_C$ ,  $n_i$  is the fraction of occupancy of the  $i$ -th atomic shell,  $C_i$  is the nuclear shape factor,  $\beta_i$  is the Coulomb amplitude of the electron radial wave function (essentially, the modulus of the wave function at the origin) and  $B_i$  is an atomic correction for electron exchange and overlap. Note that in eq.(1) there is a dependence on the neutrino mass for any single contribution in the sum.

### *Inner Bremsstrahlung end-point*

In beta decays, the neutrino mass can be measured because of the presence, in the rate, of the phase space factor for the antineutrino:  $E_{\nu} \cdot p_{\nu} \simeq (Q - E_e) \cdot \sqrt{(Q - E_e)^2 - m_{\nu}^2}$ . An analogous factor appears in the expressions for the rate of IBEC (where the electron energy is replaced by the emitted photon energy) and of the EC decay with Auger electron emission. So far, only one experiment measured the  $^{163}\text{Ho}$  IBEC spectrum, but the sensitivity at the end-point was impaired by background [23].

### Calorimetric absorption spectrum end-point

In a calorimetric experiment the same neutrino phase space factor appears, with the total de-excitation energy replacing the energy of the electron. Although at a first glance the calorimetric spectrum for EC decays may appear as a series of lines at energies  $E_i$ , where  $E_i$  is the ionization energy of the captured electron, these lines have a natural width of a few eV and therefore the actual spectrum is a continuum with marked peaks (see Fig. 1). If the  $Q$ -value of the decay happens to be close to one of the  $E_i$ , the rate near to the endpoint, where the neutrino mass effects are relevant, will be greatly enhanced.

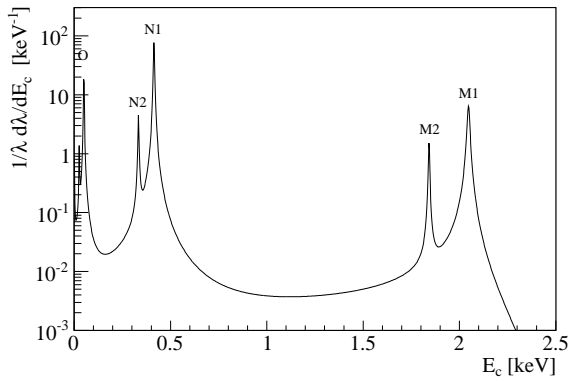


Figure 1: Expected de-excitation energy spectrum of the EC decay of  $^{163}\text{Ho}$  with  $Q = 2.5$  keV. Detector resolution effects are not included. The parameters used in the calculation are given in Section 4.

The distribution in de-excitation (calorimetric) energy  $E_c$  is expected to be

$$\frac{d\lambda_{EC}}{dE_c} = \frac{G_\beta^2}{4\pi^2} (Q - E_c) \sqrt{(Q - E_c)^2 - m_\nu^2} \times \left( 2 \right) \sum_i n_i C_i \beta_i^2 B_i \frac{\Gamma_i}{2\pi} \frac{1}{(E_c - E_i)^2 + \Gamma_i^2/4}, \quad (2)$$

an expression derived in ref.[16], where numerical checks to test the validity of the approximations made were also presented. As one can see, the very heights of the peaks in the energy distribution depend on the neutrino mass. The dependence is however too weak - for  $Q$ -values around 2.5 keV - to allow its determination.

To date there are only three calorimetric absorption measurements reported in the literature:

1. the ISOLDE collaboration used a Si(Li) detector with an implanted source [24];
2. Hartman and Naumann used a high temperature proportional counter with organometallic gas [21];
3. Gatti et al. used a cryogenic calorimeter with a sandwiched source [17].

However, none of these experiments had the sensitivity required for an end-point measurement and therefore they all gave results in terms of capture rate ratios. The most evident limitations of these experiments were statistics and energy resolution. One further serious trouble for the Si(Li) and cryogenic detectors was incomplete energy detection caused by implant damages and weak thermal coupling of the source, respectively.

Despite the shortcomings of previous calorimetric experiments, and theoretical and experimental uncertainties, a calorimetric absorption experiment seems the only way to achieve sub-eV sensitivity for the neutrino mass. Moreover, cryogenic microcalorimeters have reached the necessary maturity to be used in a large scale experiment with good energy and time resolution and are therefore the detector of choice for a sub-eV Holmium experiment.

### 3. A roadmap for a Holmium Experiment

The road to achieve a sensitivity on the electron neutrino mass of  $0.1 \text{ eV}/c^2$  and beyond can be divided into two parts. The first one is the demonstration of the feasibility of such an experiment, the second one is the actual design and construction. In this section we discuss the steps necessary to demonstrate the feasibility of a Holmium experiment, while in the next we will focus on the actual experiment requirements. We have identified four major steps necessary to demonstrate the feasibility of a Holmium experiment, we discuss them in details in the following subsections.

#### 3.1. The $Q$ -value of the decay

The statistical sensitivity of the  $^{163}\text{Ho}$  spectrum to the mass of the electron neutrino is strongly dependent on the  $Q$ -value of the reaction. The smaller the  $Q$ -value (and thus closer to the energy of the M-peak) the more sensitive the experiment will be. As discussed before, at this time the  $Q$ -values obtained by means of the capture ratios are affected by large uncertainties both because of the error on the theoretical atomic physics factors involved and because of the correlation with the neutrino mass. The various  $Q$  determinations span from 2.2 to 2.8 keV and the current recommended value is  $2.555 \pm 0.016$  keV [25].

The first necessary step in the desing and implementation of a Holmium experiment is an accurate, calorimetric measurement of the  $Q$ -value. The easiest, and most straightforward way to measure it is using a cryogenic microcalorimeter similar to the one suggested for the full implementation of the experiment. Due to the

looser constraints of the measurement, however, a single detector would be sufficient and the requirements on energy resolution could be significantly relaxed. The statistics necessary to establish with high accuracy the end-point of the full calorimetric spectrum depends on the  $Q$ -value itself. Using a detector with energy resolution of 10 eV, about  $5 \times 10^5$  counts would be sufficient to determine the spectrum end-point with an accuracy better than 20 eV for any  $Q$ -value between 2.2 and 2.8 keV. Notice that, for reasonable count rates (less than 100 counts/s) the measured  $Q$ -value is not significantly affected by the detector pileup, so the total statistics can be translated directly to a total time.

### 3.2. $^{163}\text{Ho}$ Production

$^{163}\text{Ho}$  was discovered at Princeton in 1968 in a sample of  $^{162}\text{Er}$  that was neutron activated in a nuclear reactor. Since its discovery,  $^{163}\text{Ho}$  has been produced in laboratory only for the purpose of nuclear and atomic property study. Since  $^{163}\text{Ho}$  is not available off the shelf, a dedicated process must be set up to produce the amount needed by a neutrino mass experiment. The most challenging issue is the achievement of the very high level of radio-purity required. There are a few processes that are appealing for the intrinsic  $^{163}\text{Ho}$  production rate as compared to the accompanying production of radioactive contaminants. The most interesting ones are:

- neutron activation in nuclear reactor of  $^{162}\text{Er}$  [ $^{162}\text{Er}(n,\gamma)^{163}\text{Er}(75\text{min}) \rightarrow ^{163}\text{Ho}$ ] with a cross section  $\sigma$  of about 180 barns;
- alpha particle bombardment of  $^{165}\text{Ho}$  target [ $^{165}\text{Ho}(^4\text{He},*)^{163}\text{Ho}$ ] with a  $\sigma$  of about 0.05 barns at 55 MeV;
- gamma bombardment of  $^{165}\text{Ho}$  target [ $^{165}\text{Ho}(\gamma,2n)^{163}\text{Ho}$ ] with a  $\sigma$  of about 0.14 barns at 17 MeV.

The highest production rate is achievable with the neutron activation of  $^{162}\text{Er}$ , even if to the detriment of contemporaneous built-up of very short half-life contaminants in the sample. The reactions with high energy projectiles have cross section thousands of times lower and therefore require higher intensity beams and longer activation times. On the other hand, they can use natural Holmium as target and have a highly suppressed contaminant production. Production of  $^{163}\text{Ho}$  with the neutron activation of  $^{162}\text{Er}$  requires a detailed investigation of the process, because not all cross sections are fully known: a trade-off among reproducibility, easiness

of the operations, production rate and radioactive background must be sought.

A first very preliminary test of neutron activation of  $^{162}\text{Er}$  38% enriched sample of erbium oxide has been already done by some of the authors. The irradiated sample, after waiting one month for the decay of the activity of short-lived isotopes, was first dissolved in a HCl solution and then deposited onto a Transition Edge Sensor (TES) microcalorimeter to be operated at 0.1 K at the University of Genova. The measured spectrum shows that  $^{163}\text{Ho}$  was indeed produced although it is impossible to estimate the background. The solution was analyzed by Inductively Coupled Plasma Mass Spectrometry (ICP-MS) at the University of Milano-Bicocca and the presence of  $^{163}\text{Ho}$  was confirmed.

A large scale irradiation has also just been completed at the 1 MW Portuguese Research Reactor (RPI) at the Nuclear and Technological Institute, Instituto Superior Técnico (IST-ID) in Lisbon. This reactor has a thermal column with average thermal and epithermal neutron fluxes of about  $3 \times 10^{13} \text{ cm}^{-2} \text{ s}^{-1}$  and  $3.7 \times 10^{11} \text{ cm}^{-2} \text{ s}^{-1}$ , respectively. The estimated  $^{163}\text{Ho}$  production rate is about 3 kBq/mg( $^{162}\text{Er}$ )/week (assuming the reactor is running 12 hours/day and 5 days/week).

Purification and oxide reduction of Ho to metal can proceed as follows. First, three steps of cation-exchange column separation are carried out in order to absorb the rare earths and wash out the other impurities. Then, Ho is removed with Ethylenediaminetetraacetic acid (EDTA) and  $\text{HNO}_3$  in multiple step processes. The resulting sample is mixed in a compounds for thermal reduction of Ho oxide. The final sample will be compound with metal Ho in low concentration, suitable as a target material for the following steps aiming at embedding the  $^{163}\text{Ho}$  in the detectors.

### 3.3. Detector Performance

After 30 years from their introduction [26, 27], cryogenic microcalorimeters are a mature and reliable technology used in many applications, including neutrino experiments. Detectors with the proper energy resolution and speed for the proposed investigation already exist, however, they must be designed and optimized for the requirements of a Holmium experiment. We discuss here the principal characteristics of microcalorimeters and their relevance to a Holmium experiment.

Microcalorimeters are composed of three parts, an absorber that converts energy into heat, a thermometer (or sensor) that detects the temperature variations of the absorber and a weak thermal link between the detector and a heat sink. When energy is released in the absorber,

the temperature of the detector first rises and then returns to its original value due to the weak thermal link to the heat sink. The temperature change is proportional to the energy and is detected by the thermometer. Resistive thermometers (i.e., thermometers whose resistance changes with temperature) have been the primary choice in many applications for years, but magnetic and kinetic inductance thermometers have also, more recently, demonstrated high performance [28, 29, 30, 31].

In designing a neutrino experiment, three characteristics of microcalorimeters must be considered: energy resolution, rise time of the events, and decay time. The effect of the energy resolution on the outcome of a neutrino experiment is obvious (better resolution implies better accuracy), and it is quantified in section 4. The energy resolution of a microcalorimeter is noise limited and independent of the energy being detected. It depends on the heat capacitance  $C$  of the detector, the temperature  $T$ , and the sensitivity of the thermometer  $\alpha$ , according to the expression [32]:

$$\Delta E \propto \sqrt{\frac{k_B C T}{\alpha}}, \quad (3)$$

where  $k_B$  is the Boltzmann constant. It is clear from the expression that, to obtain good energy resolution, it is important to work with small objects and material with low specific heat (to keep the heat capacitance low), at low temperature, and with sensitive thermometers. Current technology has already achieved energy resolution below 2 eV FWHM, using both TES and magnetic thermometers [33]. Both technologies are currently considered for a Holmium experiment. However, to use them for the measurement of the electron neutrino mass, the  $^{163}\text{Ho}$  radioactive isotope must be embedded in the detector for a fully calorimetric measurement. Different procedures to embed the  $^{163}\text{Ho}$  in the detector are being investigated, and tests to verify that they do not significantly affect the detector performance are underway.

The rise time is the time it takes for the signal to change in response to the energy release. This time is, in principle, the time needed for the thermometer temperature to rise and is determined by heat diffusion in the absorber and the thermal coupling between absorber and thermometer. However, in many practical applications such time is quite fast and the rise time is limited, instead, by the response time of the readout electronics. The event's rise time is perhaps the most important parameter in a Holmium experiment as it affects directly the fraction of unresolved pileup events. If a second energy release happens within the rise of a previous one, the two events may look like a single event of higher energy. The ensemble of such events generates

a second energy spectrum (unresolved pileup spectrum) which has significant statistics in the region of interest for the neutrino mass ( $Q$ -value region), and acts as a strong background component. Although the shape of the pileup spectrum can be accurately modeled, the statistical uncertainty on the number of unresolved pileup events can easily be the stronger limit on the neutrino mass sensitivity. A significant effort is ongoing in order to develop analysis algorithms to identify and eliminate such events. However, although we can now identify double events significantly closer than the rise time [34], in the end any Holmium experiment must be designed with the smallest possible rise time to minimize pileup events. Rise times of a few micro-seconds are typical for TES microcalorimeters (limited by the readout electronics), while they can be significantly shorter for magnetic microcalorimeters.

The decay time is the time it takes for the signal to return to the initial level in order that the detector be ready to register another event. An event happening on the decay of a previous one is usually easily identifiable, and does not contribute to the unresolved pileup spectrum. However, due to detector's non-linearities, both events must be discarded, contributing to the detector dead time. TES microcalorimeters have typical decay times below a millisecond, making the dead time negligible for count rates up to hundred of counts per second. However, magnetic microcalorimeters could have much longer decay times, and the count rate may become an issue. Magnetic penetration thermometers (MPT)[35] use the same geometry as magnetic thermometers but replaces the magnetic material with a superconductor in its transition. MPTs potentially combine the best of the magnetic calorimeter and TES technologies, providing the sensitivity of a TES in a dissipationless configuration [36].

Particular attention in a neutrino experiment must also be given to the readout electronics. Both TES and magnetic microcalorimeters are read out using Superconducting Quantum Interference Devices (SQUID). The direct approach of using individual readout channels for each detector has the necessary performance required by a Holmium experiment. However, considering the number of detectors involved, such approach may not be practical. Fortunately, the same issues affect several other investigations, and a massive effort on different SQUID multiplexing schemes is going on in laboratories around the World. These include time division multiplexing, frequency division multiplexing, code division multiplexing, and microwave multiplexing [37]. Kinetic inductance detectors also offer a natural path to microwave multiplexing.

### 3.4. Theoretical Uncertainties

In spite of the many experiments, atomic and nuclear details of the  $^{163}\text{Ho}$  decay are still affected by some uncertainty. The natural width of the atomic levels involved in the atomic cascade following the EC is not directly known. Moreover, the expected total absorption spectrum shape is not completely established. Riisager [38] pointed out that the spectrum predicted in [16] is only a first approximation because the rate at the end-point may be altered by the broadness of atomic level which affects the phase space available to atomic transitions. It is, however, important to note that the *shape* of the energy distribution near its endpoint is bound to be determined by the value of the neutrino mass, even if the rate itself may be uncertain because of the poor knowledge of atomic parameters.

It has also been observed [39] that the ionization energies of interest in our equations differ from those obtained by Dysprosium excitation because of the presence of a further  $N_{6,7}$  electron: those parameters will be measured with precision from the positions of the peaks in the  $E_c$  distribution. A high statistics and high energy resolution measurement of the total absorption spectrum is therefore a prerequisite for a neutrino mass measurement using the end-point as proposed in [16].

## 4. A Holmium Experiment

In this section we discuss how the statistical sensitivity depends on the main experimental parameters. We then translate this in the experimental configurations required for a sub-eV sensitivity.

The analysis is carried out using a frequentist Monte Carlo code developed to estimate the statistical sensitivity of a neutrino mass experiment performed with thermal calorimeters [11]. The approach is to simulate the energy spectra that would be measured by a large number of experiments carried out in a given configuration: the spectra are then fitted as the real ones and the statistical sensitivity is determined from the distribution of the obtained neutrino mass square,  $m_\nu^2$  [11].

The Monte Carlo parameters for the simulated experimental configuration are the total statistics  $N_{ev}$ , the FWHM of the detector energy resolution  $\Delta E_{\text{FWHM}}$  and the fraction of unresolved pile-up events  $f_{pp}$ . The simulated energy spectrum is then given by

$$S(E) = \frac{N_{ev}}{\lambda_{EC}} \int_0^{2(Q-m_\nu)} dE_1 R(E - E_1) \cdot \left[ \frac{d\lambda_{EC}}{dE_c}(E_1) + \frac{f_{pp}}{\lambda_{EC}} \int_0^{E_1} dE_2 \frac{d\lambda_{EC}}{dE_c}(E_2) \right],$$

$$\frac{d\lambda_{EC}}{dE_c}(E_1 - E_2) \Big], \quad (4)$$

where  $d\lambda_{EC}/dE_c$  is given in (2) and the response function  $R(E)$  is assumed to have a gaussian form

$$R(E) = \frac{1}{\sigma \sqrt{2\pi}} \exp\left(-\frac{E^2}{2\sigma^2}\right) \quad (5)$$

with standard deviation  $\sigma = \Delta E_{\text{FWHM}}/2.35$ . The input parameters are linked to the ones actually characterizing a real experiment:  $N_{ev} = N_{det} A_\beta t_M$  and  $f_{pp} \approx A_\beta \tau_R$ , where  $N_{det}$  is the number of detectors,  $A_\beta$  is the EC activity of a single detector,  $t_M$  is the live time of the experiment, and  $\tau_R$  is the pile-up resolving time (i.e., the minimum time separation between events that can be distinguished).

The free parameters in the fitting of the simulated spectra with Eq. (4) are the total statistics  $N_{ev}$ , the fraction of pile-up events  $f_{pp}$ , the EC transition  $Q$ -value and the squared neutrino mass  $m_\nu^2$ . The  $^{163}\text{Dy}$  atomic parameters  $E_i$ ,  $\Gamma_i$  and  $\beta_i^2$  used for the numerical evaluation of (2) are considered known and therefore fixed to the values shown in Tab. 1. The levels of the electrons that

Table 1: Energy levels of the captured electrons, with their widths, for  $^{163}\text{Dy}$  [40]. Electrons squared wave functions at the origin  $\beta_i^2$  relative to  $\beta_{M_1}^2$  [41].

Level	$E_i$ [eV]	$\Gamma_i$ [eV]	$\beta_i^2/\beta_{M_1}^2$
M <sub>1</sub>	2047	13.2	1.0
M <sub>2</sub>	1842	6.0	0.0526
N <sub>1</sub>	414.2	5.4	0.2329
N <sub>2</sub>	333.5	5.3	0.0119
O <sub>1</sub>	49.9	3.0	0.0345
O <sub>2</sub>	26.3	3.0	0.0015

can be captured are fully occupied (i.e.  $n_i = 1$ ) and the exchange and overlap corrections  $B_i$  are neglected (i.e.  $B_i \sim 1$ ).<sup>1</sup>

Given the large uncertainties on the  $Q$ -value, the Monte Carlo study has been carried out for a set of reasonable values, i.e. 2200, 2400, 2600 and 2800 eV.

From Fig. 2 it can be appreciated how the total statistics  $N_{ev}$  is crucial to reach a sub-eV neutrino mass statistical sensitivity. The fine dashed line on the plot corresponds to a  $N_{ev}^{-1/4}$  functional dependence of the sensitivity as it would be naively expected for a  $m_\nu^2$  sensitivity purely determined by statistical fluctuations. A

<sup>1</sup>They are not given for all the levels needed in [22]. Those given differ from unity by less than  $\sim 10\%$ . The validity of this approximation far from the peaks may be doubted, however the *shape* of the spectrum near to the end-point is anyhow determined by the neutrino phase-space factor.

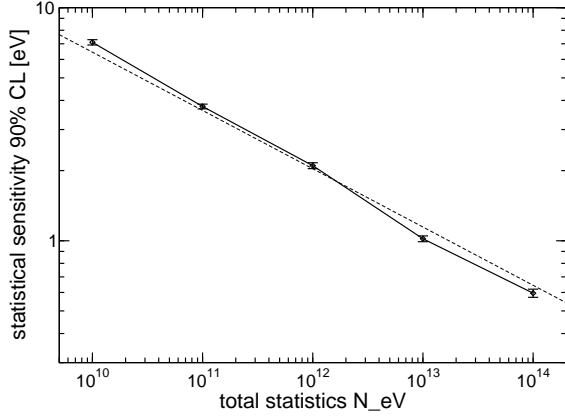


Figure 2:  $\Delta E_{FWHM} = 1$  eV,  $f_{pp} = 10^{-5}$ ,  $Q = 2600$  eV.

more detailed analysis of the sensitivity as a function of the statistics, for different pile-up fractions  $f_{pp}$  and  $Q$ -values, shows that it can be interpolated as  $N_{ev}^{-1/\alpha}$ , with  $\alpha$  between 3.3 and 4.0: in the following we conservatively use  $N_{ev}^{-1/4}$  to scale the Monte Carlo results.

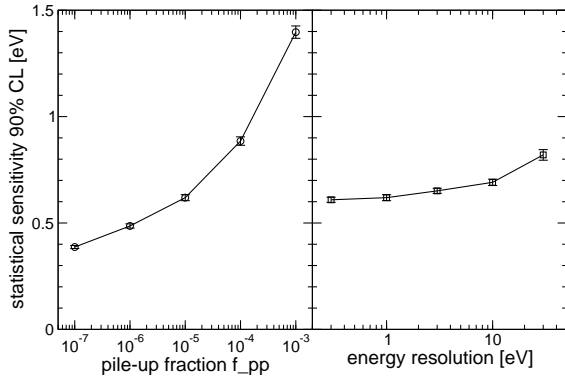


Figure 3:  $N_{ev} = 10^{14}$ ,  $\Delta E_{FWHM} = 1$  eV,  $Q = 2600$  eV (left).  $N_{ev} = 10^{14}$ ,  $f_{pp} = 10^{-5}$ ,  $Q = 2600$  eV (right)

Fig. 3 shows the effect of both the energy resolution  $\Delta E_{FWHM}$  and the fraction of pile-up events  $f_{pp}$  on the neutrino mass statistical sensitivity. As far as the energy resolution  $\Delta E_{FWHM}$  is concerned, in the typical range accessible with today's microcalorimeter technology, its impact on the sensitivity of a Holmium experiment is clearly small.

On the contrary, the increase of  $f_{pp}$  has a strong effect on the sensitivity. However it may pay out to increase the single pixel activity  $A_\beta$ , even if this entails an increased fraction of unresolved pile-up events  $f_{pp}$ . This is demonstrated by Fig. 4, where the statistical sensitiv-

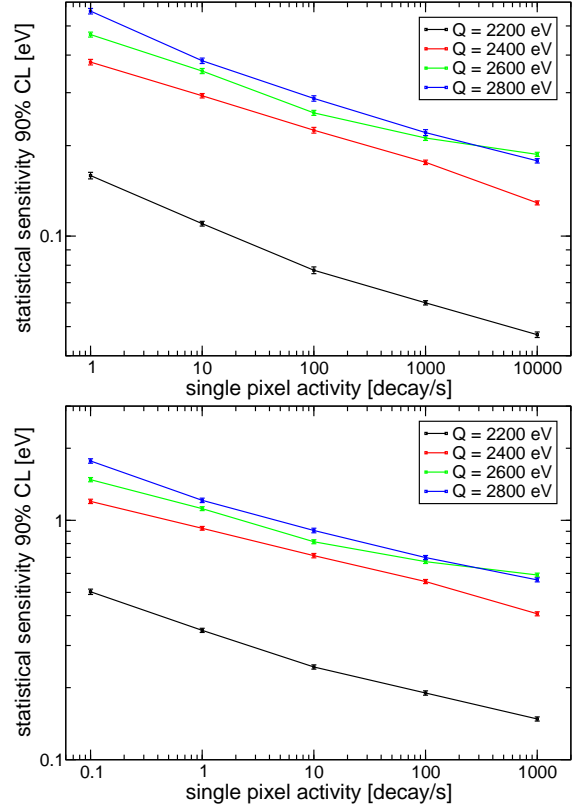


Figure 4:  $\Delta E_{FWHM} = 0.3$  eV,  $\tau_R = 0.1 \mu s$ ,  $T = 10^6$  detector $\times$ year (top).  $\Delta E_{FWHM} = 1$  eV,  $\tau_R = 1 \mu s$ ,  $T = 10^5$  detector $\times$ year (bottom).

ity is plotted as a function of the single pixel activity  $A_\beta$ , for given pile-up resolving time  $\tau_R$  and experimental exposure  $T = N_{det} t_M$  (with  $N_{ev} = A_\beta T$ ). Despite the higher fraction of unresolved pile-up events, the increase in pixel activity  $A_\beta$  directly increases the experiment statistics for a given measuring time and the overall result is an improvement in the sensitivity of the experiment. It is worth recalling here that about  $2 \times 10^{11}$   $^{163}\text{Ho}$  nuclei are needed for an activity of about 1 decay/s.

Fig. 4 also shows how the sensitivity depends on the transition  $Q$ -value. While the sensitivity is clearly much better for a  $Q$ -value of 2200 eV, higher values result in quite similar sensitivities. In particular, because of the peculiar peaky shape of the pile-up spectrum in the 2200–2600 eV interval (see Fig. 5), for high pile-up rates the sensitivity is not monotonically improving when lowering the  $Q$ -value.

In Fig. 4 two possible experimental configurations are considered. The lower panel refers to an experiment running arrays with today state-of-the-art thermal

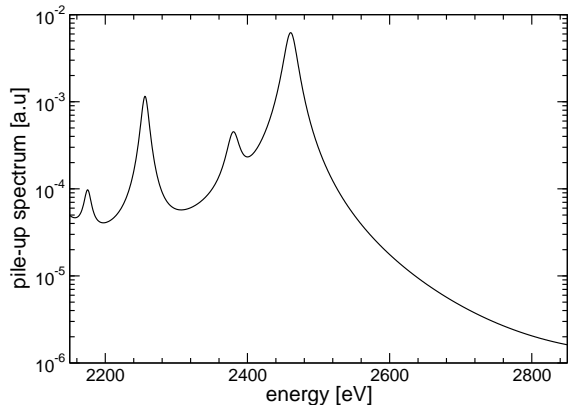


Figure 5: Pile-up spectrum.

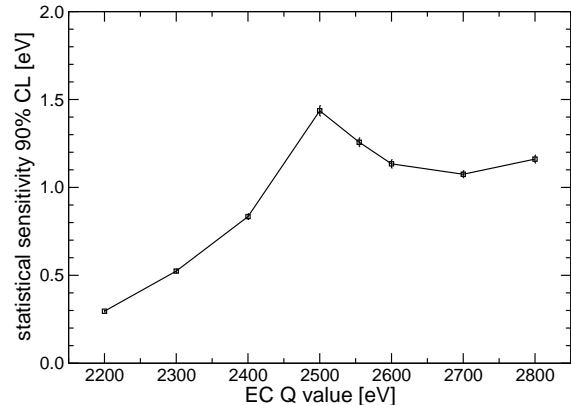


Figure 6: Pilot experiment sensitivity.

Table 2: Experimental exposure required for various target statistical sensitivities, with  $b = 0$  and two different sets of detector parameters. Configuration A is with  $\Delta E_{\text{FWHM}} = 1$  eV,  $\tau_R = 1$   $\mu$ s and  $A_\beta = 1000$  Hz. Configuration B is with  $\Delta E_{\text{FWHM}} = 0.3$  eV,  $\tau_R = 0.1$   $\mu$ s and  $A_\beta = 10000$  Hz.

$Q$ [eV]	target sensitivity [eV]	exposure $T$ [detector $\times$ year]	
		Conf. A	Conf. B
2200	0.2	$2.6 \times 10^4$	$3.3 \times 10^3$
2200	0.1	$4.1 \times 10^5$	$4.8 \times 10^4$
2200	0.05	$6.6 \times 10^6$	$7.7 \times 10^5$
2800	0.2	$6.5 \times 10^6$	$6.3 \times 10^5$
2800	0.1	$1.0 \times 10^8$	$1.0 \times 10^7$
2800	0.05	$1.7 \times 10^9$	$1.6 \times 10^8$

microcalorimeter technology: the experimental exposure is  $10^5$  detector $\times$ year which, for example, could be achieved measuring for 10 years arrays with a total of  $10^4$  pixels. The upper panel considers a more aggressive configuration with a factor 10 higher exposure and detectors with better energy and time resolution.

To conclude, in Tab.2 we have evaluated the experimental exposure required to reach target neutrino mass statistical sensitivities of 0.2, 0.1 and 0.05 eV for two different sets of detector parameters (comparable to those in Fig. 4) and for the two extremes of the  $Q$ -value range.

On a short time scale, a smaller size pilot experiment may be carried out with the aim of testing the potential of a Holmium experiment. Fig. 6 shows the  $m_\nu$  statistical sensitivity achievable for total statistics of about  $8.5 \times 10^{13}$  events, using detectors with an energy and time resolution of 1.5 eV and 1  $\mu$ s, respectively, each

with an  $^{163}\text{Ho}$  activity of about 300 decay per second. This exposure could be obtained for example by running 3000 detectors for about 3 years. The sensitivities in Fig. 6 have been estimated for  $Q$ -values in the 2200–2800 eV range and span from about 0.3 to about 1.5 eV.

## 5. Conclusions

The absolute value of the neutrino masses is not yet known. The most stringent upper limits on them come from experiments on tritium beta decay with electrostatic spectrometers: the best limit of sensitivity to which this technique can be pushed in the future seems to be  $\sim 0.2$  eV, as in the KATRIN experiment [8]. A completely different technique using cryogenic microcalorimeters to perform a calorimetric experiment has been proposed and applied in pilot experiments measuring the beta decay of the isotope  $^{187}\text{Re}$ , which has a very low  $Q$ -value but also a very long lifetime, and a large experiment, MARE [10], will follow this path.

The technique has in fact reached a maturity that allows to envisage a full scale experiment in order to reach an even better sensitivity. In this paper, we have presented the roadmap to reach this goal in a calorimetric experiment using the electron capture in  $^{163}\text{Ho}$  - an isotope having similar  $Q$ -value but much shorter lifetime - to obtain a limit on the electron neutrino mass, following a suggestion made many years ago [16]. This paper shows that such an experiment is clearly challenging, but doable, and we identified a clear path and technical steps necessary for its success.



## Acknowledgements

The authors would like to thank Dr. Ezio Previtali, Dr. Massimiliano Clemenza, and Dr. Andreas Kling for their support.

## References

- [1] see, for instance,  
G.L. Fogli *et al.*, Nucl. Phys. Proc. Suppl. **188** (2009) 27.  
M. C. Gonzalez-Garcia *et al.*, JHEP **04** (2010) 056.
- [2] G. Mention *et al.*, Phys. Rev. **D83** (2011) 073006.  
arXiv:1101.2755  
D. Boyanovsky, H. J. de Vega, N. Sanchez, Phys. Rev. **D77** (2008) 043518. arXiv:0710.5180.
- [3] W. Hu, D. J. Eisenstein, and M. Tegmark, Phys. Rev. Lett. **80** (1998) 5255.
- [4] S. Hannestad, Rep. Prog. Phys. **65** (2010) 185-208. and references therein.
- [5] E. Fermi, Z. Physik **88** (1934) 161.  
E. W. Otten, C. Weinheimer, Rep. Prog. Phys. **71** (2008) 086201. arXiv:0909.2104
- [6] F. T. Avignone III, S. R. Elliott, J. Engel, Rep. Prog. Phys. **80** (2008) 481-516. arXiv:0708.1033
- [7] Ch. Kraus *et al.*, Eur. Phys. J. **C40** (2005) 447.  
V. M. Lobashev, Nucl. Phys. **A719** (2003) 153c.  
V. N. Aseev, arXiv:1108.5034v1 [hep-ex]
- [8] KATRIN Design Report (2004), FZKA7090  
KATRIN LoI (2001), hep-ex/0109033
- [9] M. Galeazzi *et al.*, Phys. Rev. **C63** (2001) 014302.  
F. Gatti *et al.*, Nucl. Phys. **B91** (2001) 293  
C. Arnaboldi *et al.*, Phys. Rev. Lett. **91** (2003) 161802.  
M. Sisti *et al.*, Nucl. Inst. and Meth. **A520** (2004) 125.
- [10] the MARE proposal, <http://mare.dfm.uninubria.it>  
E. Andreotti, *et al.*, Nucl. Instr. Meth. Phys. Res. A **572** (2007) 208.  
A. Nucciotti, proceeding of Neutrino 2010, Athens, Greece, June 14-19, 2010, arXiv:1012.2290v1
- [11] A. Nucciotti *et al.*, Astropart. Phys. **34** (2010) 80
- [12] C. L. Bennett *et al.*, Phys. Lett. **B107** (1981) 19.
- [13] A. De Rújula, Nucl. Phys. **B188** (1981) 414.
- [14] B. Jonson *et al.*, Nucl. Phys. **A396**, 479 (1983);  
H. L. Ravn *et al.*, AIP Conf. Proc. **99**, 1-16 (1983).
- [15] A. De Rújula, M. Lusignoli, Nucl. Phys. **B219** (1983) 277.
- [16] A. De Rújula and M. Lusignoli, Phys. Lett. **B118** (1982) 429.
- [17] F. Gatti *et al.*, Phys. Lett. **B398** (1997) 415.
- [18] F. Gatti *et al.*, J. Low Temp. Phys. **151** (2008) 603.
- [19] P. C.-O. Ranitzsch *et al.* J. Low Temp. Phys., Online First (2012).
- [20] J. U. Andersen *et al.*, Phys. Lett. **B113** (1982) 72  
P. A. Baisden *et al.*, Phys. Rev. **C28** (1983) 337-341  
S. Yasumi *et al.*, Phys. Lett. **B334** (1994) 229-233.
- [21] F. X. Hartmann, R. A. Naumann, Nucl. Instrum. Meth. **A313** (1992) 237-260.
- [22] W. Bambynek *et al.*, Rev. Mod. Phys. **49** (1977) 77 [Erratum-  
ibid. **49** (1977) 961].
- [23] P. T. Springer, C. L. Bennett, P. A. Baisden, Phys. Rev. **A35** (1987) 679. in eq.(1)
- [24] H. L. Ravn *et al.*, In \*La Plagne 1984, Proceedings, Massive Neutrinos In Astrophysics and In Particle Physics\*, 287-294.
- [25] C. W. Reich and B. Singh, Nuclear Data Sheets **111** (2010) 1211;  
G. Audi and A. H. Wapstra, Nucl. Phys. **A595** (1995) 409.
- [26] S. H. Moseley, J. C. Mather and D. McCammon, J. of Appl. Phys. **56** (1984) 1257.
- [27] E. Fiorini and T. O. Niinikoski, Nucl. Instr. Meth. Phys. Res. A **224** (1984) 83.
- [28] B. Cabrera, J. Low Temp. Phys. **151** (2008) 82.
- [29] R. L. Kelley *et al.*, J. Low Temp. Phys. **151** (2008) 375.
- [30] B. A. Mazin, Microwave Kinetic Inductance Detectors: The First Decade, Aip. Conf. Proc. **1185** (2009) 135.
- [31] A. Fleischmann *et al.*, Aip. Conf. Proc. **1185** (2009) 571.
- [32] M. Galeazzi and D. McCammon, J. Appl. Phys. **93** (2003) 4856.
- [33] B. Young, B. Cabrera, and A. Miller (Editors) "The Thirteenth International Workshop on Low Temperature Detectors-LTD13", Aip. Conf. Proc. **1185** (2009).
- [34] J. D. Armstrong *et al.*, "Data analysis and Double Pulse Identification for the MARE experiment", Nucl. Instr. Meth. Phys. Res. A, in press
- [35] P. J. Shirron and M. J. DiPirro, IEEE Trans App. Sup. **3** (1993) 2140.
- [36] S. Bandler, "Magnetically Coupled Microcalorimeters", Nucl. Instr. Meth. Phys. Res. A, in press
- [37] K. D. Irwin, AIP Conf. Proc. **1185** (2009) 229
- [38] K. Riisager, J. Phys. **G14** (1988) 1301.
- [39] P. T. Springer, C. L. Bennett, P. A. Baisden, Phys. Rev. **A31** (1985) 1965.
- [40] J. A. Bearden and A. F. Burr, Rev. Mod. Phys. **39** (1967) 125 ;  
M. Cardona and L. Ley, Eds., "Photoemission in Solids I: General Principles" (Springer-Verlag, Berlin, 1978) ;  
J.L. Campbell and T. Papp, Atomic Data and Nuclear Data Tables, **77** (2001) 1.
- [41] I. M. Band and M. B. Trzhaskovskaya, Atomic Data and Nuclear Data Tables, **35** (1986) 1.